

Laplace-isospectral hyperbolic 2-orbifolds are representation-equivalent

Peter G. Doyle* Juan Pablo Rossetti†

Version 1.01 dated 1 July 2011
No Copyright‡

Abstract

Using the Selberg trace formula, we show that for a hyperbolic 2-orbifold, the spectrum of the Laplacian acting on functions determines, and is determined by, the following data: the volume; the total length of the mirror boundary; the number of cone-points of each order, counting a mirror corner as half a cone-point; and the number of primitive closed geodesics of each length and orientability class, counting a geodesic running along the boundary as half orientation-preserving and half orientation-reversing, and discounting imprimitive geodesics appropriately. This implies that Laplace-isospectral hyperbolic 2-orbifolds determine equivalent linear representations of $\text{Isom}(H^2)$, and are isospectral for any natural operator.

1 Statement

We consider compact hyperbolic 2-orbifolds M , not necessarily connected. Denote the eigenvalues of the Laplacian acting on functions on M by

$$0 = \lambda_0 \leq \lambda_1 \leq \dots$$

*Dartmouth College.

†FaMAF-CIEM, Univ. Nac. Córdoba.

‡The authors hereby waive all copyright and related or neighboring rights to this work, and dedicate it to the public domain. This applies worldwide.

We call the sequence $(\lambda_0, \lambda_1, \dots)$ the *Laplace spectrum* of M . If two spaces have the same Laplace spectrum we call them *Laplace-isospectral*. (Note that we don't simply call them 'isospectral', because this term is used in different ways by different authors.)

Our goal here will be to prove:

Theorem 1. *Let M be a compact hyperbolic 2-orbifold, not necessarily connected. The Laplace spectrum of M determines, and is determined by, the following data:*

1. *the volume;*
2. *the total length of the mirror boundary;*
3. *the number of cone-points of each order, counting a mirror corner as half a cone-point of the corresponding order;*
4. *the number of closed geodesics of each length and orientability class, counting a geodesic running along the boundary as half orientation-preserving and half orientation-reversing, and counting the k -fold iterative of a primitive geodesic as worth $\frac{1}{k}$ of a primitive geodesic of the same length and orientability.*

Of course the Laplace spectrum determines other data as well, for example the number of connected components. The data we list here determine those other data, since they determine the spectrum.

Theorem 1 can be recast less picturesquely as follows. Associated to a 2-orbifold M is a linear representation $\rho_{\bar{M}}$ of $\text{Isom}(H^2)$ on functions on the frame bundle \bar{M} of M . Associated to this representation is its character $\chi_{\bar{M}}$, a function on the set of conjugacy classes of $\text{Isom}(H^2)$. The geometrical data listed in Theorem 1 are just a way of describing geometrically the information conveyed by the character $\chi_{\bar{M}}$. Selberg tells us that the character determines the Laplace spectrum of M . This is a very general fact. What Theorem 1 tells us that is special is that for hyperbolic 2-orbifolds, we can get back from the Laplace spectrum to the character.

Once we have the character, we get by general principles the linear equivalence class of the representation $\rho_{\bar{M}}$, hence the title, 'Laplace-isospectral hyperbolic 2-orbifolds are representation-equivalent'. We also get the spectrum of any natural operator on any natural bundle. We will discuss these matters further in 9 below; for now we concentrate on Theorem 1.

2 Plan

This paper is rather longer than you might think it needs to be, even if you disregard the large Appendix. As we observed in [5], this theorem for orbifolds is a short step from the result about manifolds proven there. We carry on at such length because we are hoping to sell readers on the usefulness of the counting kernel technique, and to provide a general background on Selberg’s methods for those not familiar with them. We also take some excursions which we hope will prove interesting.

We will begin with some examples of Theorem 1 in action; fill in the necessary background on Selberg’s method, and its particular application to what we call the *counting kernel*; outline the proof of Theorem 1; fill in details; and discuss the implications for linear equivalence and strong isospectrality. Then we’ll give examples to show how the Theorem breaks down in the flat case; show how the Selberg formula works in practice; and finish up by discussing some conjectures.

3 Examples

In this section, we give examples to show that the trade-offs between boundary and interior features that are allowed for in the statement of Theorem 1 do actually take place: Boundary corners on one orbifold may appear as cone-points on the other, while boundary geodesics may migrate to the interior.

All the examples here will be obtained by glueing bunches of congruent hyperbolic triangles. The glueing patterns arise from transplantable pairs, as described by Buser et al. [2]. In Appendix A below we reproduce a large catalog of such transplantable pairs, as computed by John Conway. We will refer to this catalog to identify specific glueing patterns.

Examples of trading boundary and interior geodesics abound. A variation on the famous example of Gordon, Webb, and Wolpert [8] yields a pair of planar hyperbolic 2-orbifolds of types $*224236$ and $*224623$, shown in Figure 1. (This is presumably the simplest pair of this kind—see Section 12 below.) Each member of the pair is glued together from 7 copies of a so-called 346 *triangle*: a hyperbolic triangle with angles $\pi/3$, $\pi/4$, $\pi/6$. The glueing pattern appears in Appendix A below as pattern 7(3).

There is no issue here with geodesics passing through the interior of any

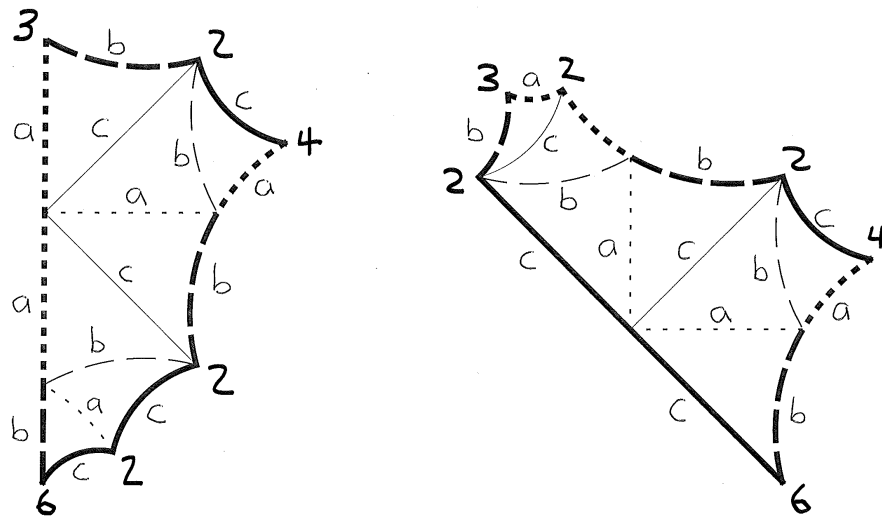


Figure 1: The pair $*224236$, $*224623$.

of the triangles that make up these two orbifolds: These can be matched so as to preserve length, orientability, and index of imprimitivity. But when it comes to geodesics that run along the edges of the triangles, whether along the mirror boundary or in the interior of the orbifold, it is necessary to balance boundary geodesics on one orbifold against interior geodesics on the other, as provided for in Theorem 1. To see this, look at Figure 1, and count geodesics on the two sides. You'll find that getting the count right is tricky, but fun. Beware that boundary geodesics turn back at corners of even order, but continue along around the boundary at corners of odd order. Beware also of the way interior geodesics bounce when they hit the boundary. The answers are indicated in Table 1. The names 'recto' and 'verso' are short for 'orientation-preserving' and 'orientation-reversing', in analogy with the names for the front and back of a printed page. The table only shows lengths for which there is at least one imprimitive geodesic. Trade-offs between boundary and interior geodesics continue at multiples of these lengths.

Examples of trading corners for cone-points are not as omnipresent as examples of trading boundary and interior geodesics, but they are still plentiful. Figures 2 and 3 show how to construct a pair $6 * 2232233, 23 * 22366$ from transplantable pair $11g(3)$ of Appendix A. Note how the order-6 cone-point moves to the boundary going one way, while the order-2 and order-3 cone-points move to the boundary going the other way. Many other examples of cone-trading can be produced using the diagrams of Appendix A, some of them much readier to hand than this one.

4 Background

Huber [9] proved the result of Theorem 1 in the case of orientable hyperbolic 2-manifolds. Huber used what would nowadays be seen as a version of the Selberg trace formula, which allows us to read off the lengths of geodesics from the spectrum in a straight-forward way. Doyle and Rossetti [5] extended the result to non-orientable hyperbolic 2-manifolds. In this case we can't simply read off the data about geodesics using the trace formula, because of interference between the spectral contributions of orientation-preserving and orientation-reversing geodesics of the same length. However, it turns out that any possible scenario for matching spectral contributions would require too many geodesics.

What we will show here is that, as we indicated in [5], it is a short step

Geodesics for *224236:

length	boundary		interior		total	
	recto	verso	recto	verso	recto	verso
$2c$	$\frac{3}{2}$	$\frac{3}{2}$			$\frac{3}{2}$	$\frac{3}{2}$
$2a + 2b$	$\frac{1}{2}$	$\frac{1}{2}$	1	1	$\frac{3}{2}$	$\frac{3}{2}$
$4c$	$\frac{3}{2} \cdot \frac{1}{2}$	$\frac{3}{2} \cdot \frac{1}{2}$	1		$\frac{7}{4}$	$\frac{3}{4}$
$4a + 4b$	$\frac{1}{2} + \frac{1}{2} \cdot \frac{1}{2}$	$\frac{1}{2} + \frac{1}{2} \cdot \frac{1}{2}$	$2 \cdot \frac{1}{2}$		$\frac{7}{4}$	$\frac{3}{4}$

Geodesics for *224623:

length	boundary		interior		total	
	recto	verso	recto	verso	recto	verso
$2c$	$\frac{1}{2}$	$\frac{1}{2}$	1	1	$\frac{3}{2}$	$\frac{3}{2}$
$2a + 2b$	$\frac{3}{2}$	$\frac{3}{2}$			$\frac{3}{2}$	$\frac{3}{2}$
$4c$	$\frac{1}{2} + \frac{1}{2} \cdot \frac{1}{2}$	$\frac{1}{2} + \frac{1}{2} \cdot \frac{1}{2}$	$2 \cdot \frac{1}{2}$		$\frac{7}{4}$	$\frac{3}{4}$
$4a + 4b$	$\frac{3}{2} \cdot \frac{1}{2}$	$\frac{3}{2} \cdot \frac{1}{2}$	1		$\frac{7}{4}$	$\frac{3}{4}$

Table 1: Counting geodesics.

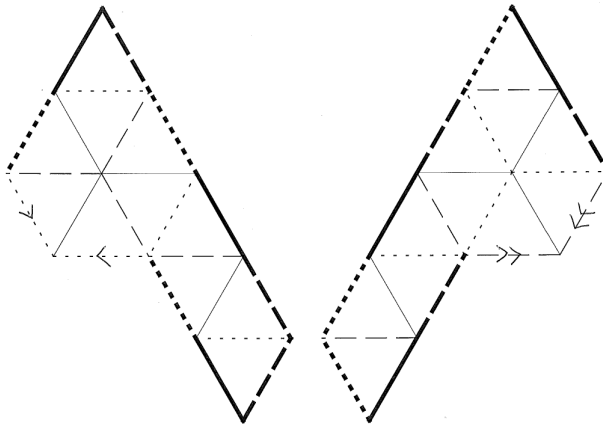


Figure 2: The transplanted pair $11g(3)$.

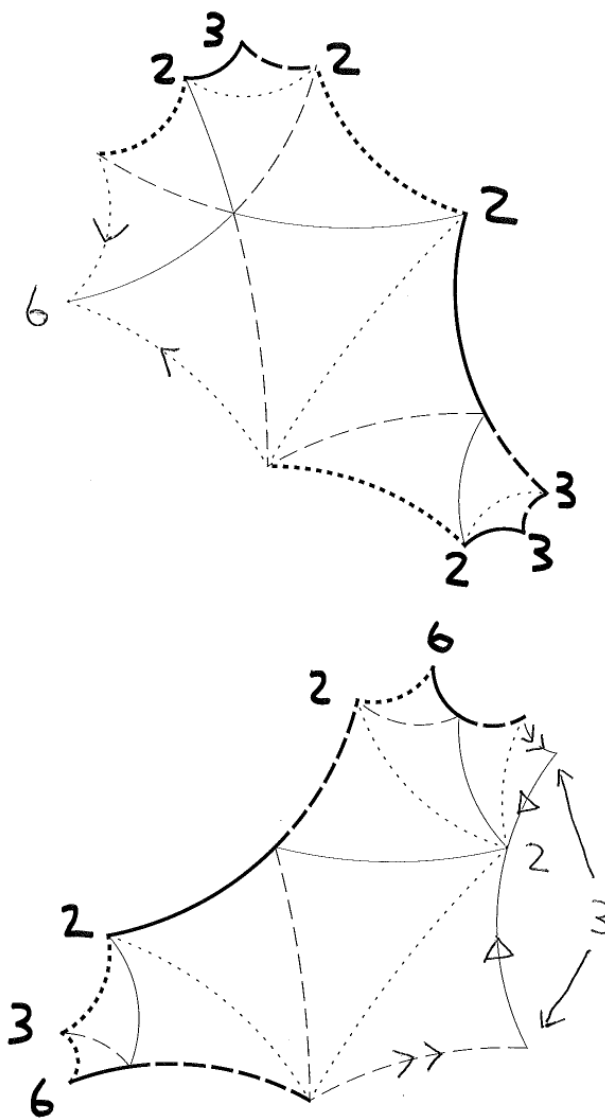


Figure 3: Replace the prototype equilateral triangle in Figure 2 by a 366 triangle so that six 3-vertices come together in the left-hand diagram. This yields a Laplace-isospectral pair of hyperbolic 2-orbifolds of types $6 * 2232233$ and $23 * 22366$.

from non-orientable surfaces to general orbifolds. The reason is that the Selberg formula permits us to read off the data about orbifold features, just as Huber read off the data about geodesics in the case of orientable manifolds. Then we have only to check that there is still no scenario for matching the spectral contributions of the geodesics.

There are other ways to approach showing that the Laplace spectrum determines the data about orbifold features. By looking at the wave trace, Dryden and Strohmaier [7] proved the result of Theorem 1 for orientable hyperbolic 2-orbifolds. While they did not consider non-orientable surfaces or orbifolds, it seems likely that wave techniques could be used to show that the Laplace spectrum determines all the orbifold data. The argument would be essentially equivalent to the argument we give here, only more complicated.

Another possible approach is via the heat equation. By looking at short-time asymptotics of the heat trace, Dryden et al. [6] got information about the singular set of general orbifolds (for example, the volume of the reflecting boundary). Their results yield information about orbifolds of variable curvature, and in any dimension. Restricted to hyperbolic 2-orbifolds, the results they state don't yield complete information about the singular set. All this information is there in the short-time asymptotics of the heat trace, however, and presumably it could be extracted using their approach, by looking at higher and higher terms in the asymptotic expansion.

The beauty of the wave and heat approaches is that they can work in great generality. The Selberg method depends on having spaces whose underlying geometry is homogeneous, such as manifolds and orbifolds of constant curvature. For studying such spaces, it is a good bet that the Selberg method will beat the wave and heat approaches. Of course, the Selberg method can be used to treat the heat and wave kernels; the bet is that you will do better to consider a simpler kernel, like the counting kernel that we use here.

5 What we need from Selberg

Here we assemble what we will need from Selberg for the proof of Theorem 1. All the ideas come from Selberg [13].

Let $G = \text{Isom}(H^2)$ be the group of isometries of H^2 . Note that G has two components, corresponding to orientation-preserving and orientation-reversing isometries. A hyperbolic 2-orbifold can be written as a union of

quotients of H^2 by discrete cocompact subgroups $\Gamma_j \subset G$, one for each connected component of M :

$$M = \cup_j \Gamma_j \backslash H^2.$$

We'll denote by $F(\Gamma_j)$ a fundamental domain for Γ_j .

In what follows, we could assume that M is connected, and write

$$M = \Gamma \backslash H^2,$$

because the extension to the disconnected case presents no difficulties. We prefer not to do this, in part to combat the common prejudice against disconnected spaces.

Define the *counting kernel* on H^2 by

$$c(x, y; s) = \begin{cases} 1, & d(x, y) \leq s \\ 0, & d(x, y) > s \end{cases}.$$

It tells when the hyperbolic distance $d(x, y)$ is at most s . Define the *counting trace*

$$\begin{aligned} C(s) &= \sum_j \int_{F(\Gamma_j)} \sum_{\gamma \in \Gamma_j} c(x, \gamma x; s) dx \\ &= \sum_j \int_{F(\Gamma_j)} \#\{\gamma \in \Gamma_j : d(x, \gamma x) \leq s\} dx. \end{aligned}$$

The counting trace tells (after dividing by the volume of M) the average number of broken geodesic loops on M of length at most s ,

The reason for the name 'counting trace' is that formally, $C(s)$ is the trace of the linear operator L_s whose kernel is the counting kernel $c(x, y; s)$ pushed down to M . L_s associates to a function $f : M \rightarrow \mathbb{R}$ the function whose value at $x \in M$ is the integral over a ball of radius s of the lift of f to the universal cover H^2 . L_s is not a actually trace class operator, because of the discontinuity of the counting kernel, but our expression for $C(s)$ is still well-defined.

We will need the following:

Proposition 1. *The Laplace spectrum determines the counting trace.*

Proof. This is a standard application of the methods of Selberg [13], which by now are ‘classical’. If you aren’t familiar with these methods, you should look at [13], or failing that, look at section 6 below. The only wrinkle here is that the kernel $c(x, y; s)$ is not continuous, so the Selberg trace formula doesn’t apply directly. One way to deal with this is to approximate by a sequence of smooth positive kernels that approach the counting kernel from above; use the trace formula to see that the Laplace spectrum determines the trace of each approximation; and then take a limit, bearing in mind that as a function of S , $C(s)$ is positive, increasing, and right-continuous. \square

The other thing we will need is the ‘other side’ of the trace formula: which will allow us to isolate the contributions to the counting trace arising from reflectors and cone-points.

Let $\text{Cl}(\gamma, \Gamma)$ denote the conjugacy class of γ in Γ , and let $Z(\gamma, \Gamma)$ denote the centralizer. We have the usual one-to-one correspondence between the set of cosets $Z(\gamma, \Gamma)\backslash\Gamma$ and the conjugacy class $\text{Cl}(\gamma, \Gamma)$, where to the coset $Z(\gamma, \Gamma)\delta$ we associate the conjugate $\delta^{-1}\gamma\delta$.

Proposition 2. *The counting trace can be expressed as a sum of contributions from conjugacy classes of Γ :*

$$C(s) = \sum_j \sum_{\text{Cl}(\gamma, \Gamma_j)} \text{Vol}(\{x \in F(Z(\gamma, \Gamma_j)) : d(x, \gamma x) \leq s\}).$$

Proof. It’s possible to visualize how this works—for a warm-up, think about the case of 1-orbifolds and flat 2-orbifolds. The trick is to group terms

belonging to the same conjugacy class:

$$\begin{aligned}
C(s) &= \sum_j \int_{F(\Gamma_j)} \sum_{\gamma \in \Gamma_j} c(x, \gamma x; t) dx \\
&= \sum_j \sum_{\gamma \in \Gamma_j} \int_{F(\Gamma_j)} c(x, \gamma x; t) dx \\
&= \sum_j \sum_{\text{Cl}(\gamma, \Gamma_j)} \sum_{Z(\gamma, \Gamma_j) \delta_{F(\Gamma_j)}} \int c(x, \delta^{-1} \gamma \delta; s) dx \\
&= \sum_j \sum_{\text{Cl}(\gamma, \Gamma_j)} \sum_{Z(\gamma, \Gamma_j) \delta_{F(\Gamma_j)}} \int c(\delta x, \gamma \delta; s) dx \\
&= \sum_j \sum_{\text{Cl}(\gamma, \Gamma_j)} \sum_{Z(\gamma, \Gamma_j) \delta_{F(\Gamma_j)}} \int c(x, \gamma x; s) dx \\
&= \sum_j \sum_{\text{Cl}(\gamma, \Gamma_j)_{F(Z(\gamma, \Gamma_j))}} \int c(x, \gamma x; s) dx \\
&= \sum_j \sum_{\text{Cl}(\gamma, \Gamma_j)} \text{Vol}(\{x \in F(Z(\gamma, \Gamma_j)) : d(x, \gamma x) \leq s\}). \quad \square
\end{aligned}$$

The virtue of this proposition is that we can evaluate the summands using simple hyperbolic trigonometry.

6 The counting trace and the Laplace spectrum

Here we extract from Selberg [13] the beautiful ideas behind the fact, so briefly disposed of in the last section, that the Laplace spectrum determines the counting trace.

We start by going in the opposite direction:

Proposition 3. *The counting trace determines the Laplace spectrum.*

Proof. Denote the heat kernel on H^2 by $k(x, y; s) = h(d(x, y), t)$. The trace of the heat kernel on M is the Laplace transform of the Laplace spec-

trum:

$$\begin{aligned} K(t) &= \sum_j \int_{x \in F_j} \sum_{\gamma \in \Gamma_j} k(x, \gamma x; t) \\ &= \sum_i e^{-\lambda_i t}. \end{aligned}$$

We can write the heat trace $K(t)$ in terms of the counting trace $C(s)$ by means of a Stieltjes integral:

$$K(t) = \int h(s, t) dC(s).$$

This is nothing more than Kelvin's method of images. So the counting trace determines the heat trace, and hence the Laplace spectrum. \square

What we will need here is the converse: The Laplace spectrum determines the counting trace. This is hardly surprising—indeed, it would be astonishing if it did not do so. That would be like discovering that you could not determine a well-behaved initial temperature distribution on a semi-infinite bar by keeping track of the temperature at the end of the bar. Heat at nearby points makes itself felt sooner, and this should be enough to allow us to solve the inverse problem, at least in principle. This isn't how our proof is going to work, and we don't know if it is possible to prove the result this way. But it should be.

The beauty and power of Selberg's approach is that it gives us a formula for how the Laplace spectrum determines the counting trace. But bear in mind that we need only the fact, not the formula.

Here, briefly, is how it works.

Consider the operator L_s that associates to a function $f : M \rightarrow \mathbb{R}$ the function whose value at $x \in M$ is the integral over a ball of radius s of the lift of f to the universal cover H^2 . This operator has kernel $c(x, y; s)$, with s fixed.

L_s commutes with the Laplacian, so we can expect to be able to choose a basis of eigenfunctions ϕ_0, ϕ_1, \dots of the Laplacian on M that are simultaneously eigenfunction for L_s :

$$\Delta \phi_i = \lambda_i \phi_i;$$

$$L_s \phi_i = \mu_i \phi_i.$$

(If you are worried that the kernel is not sufficiently smooth, approximate by a smooth function.) Selberg's great observation is that any eigenfunction ϕ of Δ on H^2 is automatically an eigenfunction for L_s : If

$$\Delta\phi = \lambda\phi$$

then

$$L_s\phi = \Lambda(\lambda)\phi,$$

where Λ is a function that is fixed, known in advance, and independent of M . (We'll give a formula for it presently.) This means that any eigenbasis for Δ on M is automatically an eigenbasis for L_s , and that the Laplace spectrum determines the spectrum (and hence the trace) of L_s .

Lemma 1 (Selberg). *For any λ and any $x_0 \in H^2$, there is a unique eigenfunction $\omega_{\lambda,x_0}(x)$ of Δ that is radially symmetric about x_0 and normalized so that $\omega_{\lambda,x_0}(x_0) = 1$.*

Proof. Write

$$\omega_{\lambda,x_0}(x) = f(d(x, x_0)),$$

and

$$\Delta\omega_{\lambda,x_0}(x) = Lf(d(x, x_0)),$$

where L is some second order differential operator that we won't bother to write down. Then we have $Lf = \lambda f$; $f(0) = 1$; $f'(0) = 0$. This determines f uniquely. (It's some kind of Bessel function.) \square

Let

$$\theta_s(\lambda) = [L_s\omega_{\lambda,x_0}](x_0),$$

and note that this doesn't depend on x_0 . (It's determined by the function we called f in the proof above.)

Theorem 2 (Selberg). *If ϕ is any eigenfunction of Δ on H^2 with eigenvalue λ , then*

$$L_s\phi = \theta_s(\lambda)\phi.$$

Note. While we've formulated this result for operators derived from the counting kernel, it applies to any kernel $k(x, y)$ depending only on the distance $d(x, y)$.

Proof. Fix x_0 . Denote by ϕ_{x_0} the result of making ϕ radially symmetric about x_0 by averaging its rotations. This symmetrization process commutes with Δ , so

$$\Delta\phi_{x_0} = \lambda\phi_{x_0}$$

and hence by the Lemma

$$\phi_{x_0} = \phi_{x_0}(x_0)\omega_{\lambda,x_0} = \phi(x_0)\omega_{\lambda,x_0}.$$

But symmetrization about x_0 does not change the integral of ϕ over a ball about x_0 , so

$$\begin{aligned} L_s\phi(x_0) &= L_s\phi_{x_0}(x_0) \\ &= [L_s\phi(x_0)\omega_{\lambda,x_0}](x_0) \\ &= \phi(x_0)[L_s\omega_{\lambda,x_0}](x_0) \\ &= \theta_s(\lambda)\phi(x_0). \quad \square \end{aligned}$$

Note. In light of result, we may say that L_s is ‘a function of the Laplacian’, and write $L_s = \theta_s(\Delta)$.

This completes the background for the proof that the Laplace spectrum determines the counting trace (Proposition 1). As we observed there, the kernel $c(x, y; s)$ is discontinuous, so the operators L_s aren’t trace class, and the formal series for $C(s)$ is not guaranteed to be absolutely convergent. To get around this, we suggested applying the trace formula to a sequence of smooth approximations to $c(x, y; s)$.

An alternative approach is to integrate the counting kernel $c(x, y; s)$ with respect to s to get the continuous kernel

$$d(x, y; s) = \begin{cases} s - d(x, y) & d(x, y) \leq s \\ 0, & d(x, y) > s \end{cases}.$$

The trace of this kernel is

$$D(s) = \int_{s=0}^s C(s).$$

Since $d(x, y; s)$ is still not smooth, the corresponding trace formula series is still not guaranteed to be absolutely convergent. But now we can approximate by smoother kernels whose traces will converge pointwise to the value of $D(s)$. (This amounts to an alternative way of summing the series for $D(s)$:

See Selberg [13, p. 68].) So the Laplace spectrum determines $D(s)$, and hence also $C(s)$.

Now, in practice the formal sum for $C(s)$ might converge pretty well with perhaps a little coddling. At least that is the case for Euclidean orbifolds—see Section 11 below.

7 Outline of the proof

The counting trace $C(s)$ is built up of contributions from the conjugacy classes of $\text{Isom}(H^2)$. The contribution from the identity is independent of s , and equal to the volume of M . The remaining conjugacy classes are of four kinds: reflections, rotations, translations, and glide reflections. Their contributions all vanish for $s = 0$, which means that $C(0)$ is the volume of M . Translations and glide reflections make no contribution for s smaller than the length of the shortest closed geodesic, so for small s the only contributions are from the identity, reflections, and rotations.

Begin by reading off the volume $C(0)$, and subtracting this constant from $C(s)$. In what is left, reflections make a contribution of first order in s , proportional to the total length of the mirror boundary. Rotations contribute only to second order, so we can read off the length of the mirror boundary, subtract out its contribution, and what is left is (for small s) entirely the result of rotations.

A simple computation now shows that the contributions of rotations through different angles are linearly independent. This allows us to read off the orders of the cone-points, and subtract out their contributions. Once we've zapped the contributions of the identity, reflections, and rotations, what is left of the counting trace vanishes identically for small s , and overall is entirely the result of translations and glide reflections, corresponding in the quotient to closed geodesics.

Here we run into the main difficulty in the proof, which is that the contributions of orientation-preserving and orientation-reversing geodesics of a given length are not linearly independent. Indeed, they are proportional, with a constant of proportionality depending on the length of the geodesic. So we can't simply read off these lengths. Fortunately, we have already established that the spectrum determines the lengths and twists of geodesics for hyperbolic 2-manifolds, (See Doyle and Rossetti [5].) and the argument carries over directly to the orbifold case, providing we take care to count geodesics along

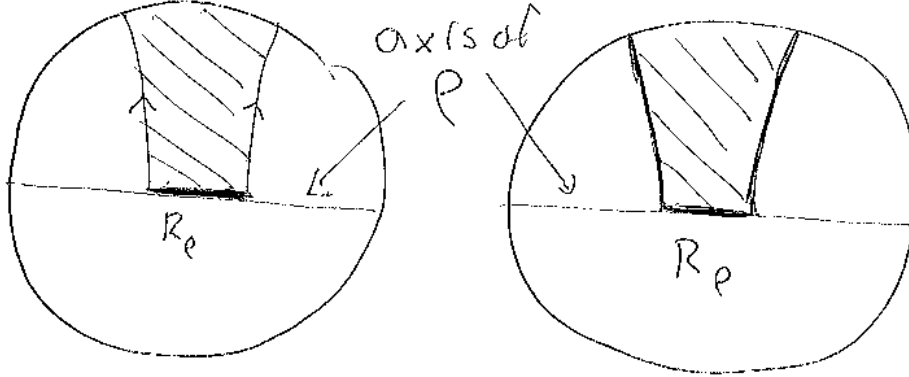


Figure 4: Possible quotients for the centralizer of a reflection.

the boundary as half orientation-preserving and half orientation-reversing.

8 Details

Denote by R the combined length of all reflecting boundaries.

Lemma 2. *The combined contribution of the reflecting boundaries to the counting trace $C(s)$ is*

$$R \sinh \frac{s}{2}.$$

Proof. Let $\rho \in \Gamma_j$ be a reflection. There are two possibilities for $Z(\rho, \Gamma_j) \backslash H^2$: a funnel or a planar domain. (See Figure 4.) In either case, the contribution to $C(s)$ is $R_\rho \sinh \frac{s}{2}$, where R_ρ is the portion of R attributable to $\text{Cl}(\rho, \Gamma_j)$, because this measures points in the quotient that are within $\frac{s}{2}$ of the axis of ρ , and hence within s of their images under the reflection ρ . (See Figure 5.) Summing over the conjugacy classes of reflections in all the groups Γ_j gives $R \sinh \frac{s}{2}$. \square

Now we turn to conjugacy classes of rotations. Each such is associated to a unique conepoint or boundary corner. From a conepoint of order n we get $n - 1$ rotations through angles $\frac{2\pi k}{n}$, $k = 1, \dots, n - 1$. For each such rotation γ the centralizer $Z(\gamma, \Gamma_j)$ is cyclic of order n , consisting of just these $n - 1$ rotations, together with the identity. The quotient $Z(\gamma, \Gamma_j)$ is (surprise!) an infinite cone of cone angle $\frac{2\pi}{n}$. For a boundary corner of angle $\frac{\pi}{n}$ the centralizer

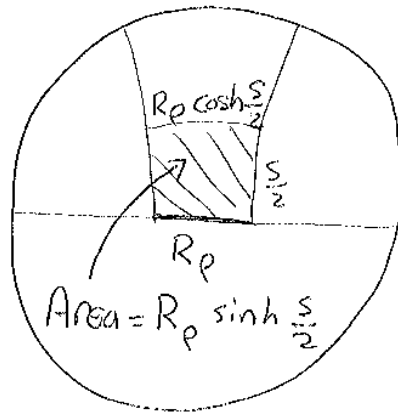


Figure 5: The contribution of a reflection to the counting trace.

is a dihedral group of order $2n$, and the quotient is an infinite sector of angle $\frac{\pi}{n}$. This quotient is half of a cone of angle $\frac{\pi}{n}$, and it should be clear that the contribution to $C(s)$ of rotations associated to a boundary corner is just half what it is for a cone-point—which is why a boundary corner counts as half a cone-point. So we can forget about boundary corners, and consider just cone-points.

Denote by $g_n(s)$ the combined contribution to the counting trace of a cone-point of order n . This contribution is the sum of the contributions of the $n - 1$ non-trivial conjugacy classes of rotations associated to the cone-point. We denote these individual contributions by $g_{k,n}(s)$:

$$g_n(s) = \sum_{k=1}^{n-1} g_{k,n}(s).$$

Lemma 3.

$$g_{k,n}(s) = \frac{1}{n} f_{\frac{2\pi k}{n}}(s),$$

where

$$f_{\theta}(s) = 2\pi \left(\sqrt{1 + \frac{\sinh^2 \frac{s}{2}}{\sin^2 \frac{\theta}{2}}} - 1 \right).$$

Proof. It should be clear that

$$g_{k,n}(s) = \frac{1}{n} f_{\frac{2\pi k}{n}}(s),$$

where $f_{\theta}(s)$ is the area $2\pi(\cosh r - 1)$ of a hyperbolic disk of such a radius r that a chord of length s subtends angle θ . (A fundamental domain for the cone hits a fraction $\frac{1}{n}$ of any disk about the center of rotation.) We just have to make sure that we have the correct formula for f_{θ} . The quantities r, θ, s satisfy

$$\sinh r = \frac{\sinh \frac{s}{2}}{\sin \frac{\theta}{2}}.$$

(See Figure 6.) Thus

$$\begin{aligned} f_{\theta}(s) &= 2\pi(\cosh r - 1) \\ &= 2\pi \left(\sqrt{1 + \sinh^2 r} - 1 \right) \\ &= 2\pi \left(\sqrt{1 + \frac{\sinh^2 \frac{s}{2}}{\sin^2 \frac{\theta}{2}}} - 1 \right). \quad \square \end{aligned}$$

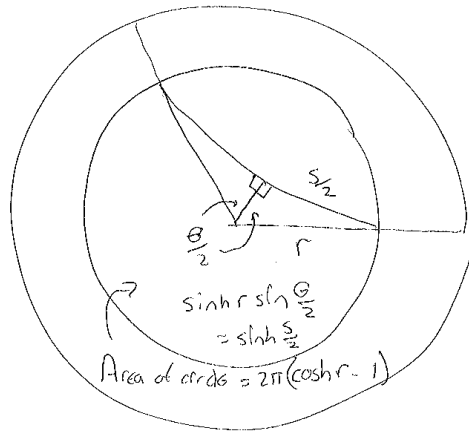


Figure 6: The circle whose chord of length s subtends angle θ

Hopefully it will seem absolutely incredible that there might be any non-trivial linear relation between these functions f_θ . There isn't:

Lemma 4. *The functions $f_\theta, 0 < \theta \leq \pi$ are linearly independent: No non-trivial linear combination of any finite subset of these functions vanishes identically on any interval $0 < s < S$.*

Proof. It suffices to show linear independence of the family of functions $\sqrt{1+au} - 1, 1 < a < \infty$, on all intervals $0 < u < U$. (Set $u = \sinh^2 \frac{t}{2}$ and $a = \frac{1}{\sin^2 \frac{\theta}{2}}$.) Actually functions of this form remain independent when a is allowed to range throughout the complex plane, and not just over the specified real interval. A quick way to see this is to write in Taylor series

$$g(u) = \sqrt{1+u} - 1 = b_1 u + \frac{b_2}{2} u^2 + \frac{b_3}{6} u^3 + \dots$$

and observe (look up?) that only the constant term vanishes:

$$b_1, b_2, \dots \neq 0.$$

If a linear combination $\sum_{i=1}^n c_i g(a_i u)$ is to vanish on $0 < u < U$, then all its derivatives must vanish at $u = 0$:

$$\sum_{i=1}^n c_i a_i^k b_k = 0, \quad k = 1, 2, \dots$$

(We ignore the constant term because all the functions involved here vanish at $u = 0$.) Dividing by b_k gives

$$\sum_{i=1}^n c_i a_i^k = 0, \quad k = 1, 2, \dots$$

Could this system of equations for c_1, \dots, c_n have a non-trivial solution? If so, then the subsystem consisting of only the first n of these equations would have a non-trivial solution:

$$\sum_{i=1}^n c_i a_i^k = 0, \quad k = 1, \dots, n.$$

Let $d_i = c_i a_i$, so that

$$\sum_{i=1}^n d_i a_i^{k-1} = 0, \quad k = 1, \dots, n.$$

The matrix (a_i^{k-1}) of this system of linear equations is a Vandermonde matrix, with determinant $\prod_{i<j}(a_i - a_j)$, so as long as the a_i are distinct the system has no non-trivial solution. \square

Note. In appealing to the fact that none of the derivatives of $\sqrt{1+u}$ happen to vanish at $u = 0$, we are seizing upon an accidental feature of the problem. We should give a more robust proof.

Proof of Theorem 1. Subtract from $C(s)$ from the counting trace the volume $C(0)$ and the contributions of the reflectors. Because of the linear independence of the functions f_{θ} , we can identify the number of cone-points of highest order. (It should go without saying that this includes the half-conepoints at boundary corners.) Subtract out their combined contribution from $C(s)$. Now we can identify the number of conepoints of the next highest order, and subtract out their contribution. Proceed until all conepoint contributions have been removed. What remains arises from the closed geodesics. In the manifold case, it is shown that the characteristics of the closed geodesics are determined by the counting trace, and hence by the spectrum. The proof carries over here essentially without change. \square

9 Implications

Caveat. The strange and infelicitous notation we use here arises from trying to handle disconnected spaces. This leads to things like considering the frame bundle of a connected orientable space to be disconnected. There could be mistakes in the notation, though hopefully not in the ideas it is meant to express.

Let $G = \text{Isom}(H^2)$ denote the group of isometries of H^2 . Note that G has two connected components, corresponding to orientation-preserving and orientation-reversing isometries. A hyperbolic 2-orbifold M can be written as a union of quotients of H^2 by discrete cocompact subgroups $\Gamma_j \subset G$, one for each connected component of M :

$$M = \cup_j \Gamma_j \backslash H^2.$$

M is naturally covered by

$$\bar{M} = \cup_j \Gamma_j \backslash G.$$

\bar{M} is the bundle of all orthonormal frames of M , not just those that have a particular orientation; every point x of M is covered by two disjoint circles

in \bar{M} , corresponding to the two orientation classes of frames of the tangent space $T_x M$. Note that there will be two connected components of \bar{M} for each orientable component of M , and one for each non-orientable component, because dragging a frame around an orientation-reversing loop (e.g. one that simply bumps off a mirror boundary) will take you from one orientation class of frames to the other.

Note. Even if M happens to be orientable, we should not think of it as oriented, because we are discussing manifolds up to isometry, not up to orientation-preserving isometry. The Laplace spectrum cannot not detect orientation, so it makes no sense to discuss oriented manifolds, and since we can't orient our manifolds, there is no obvious good reason to consider only orientable manifolds, as has commonly been done in the past when discussing isospectrality. But then again, there is no obvious good reason to consider only manifolds, as opposed to general orbifolds—possibly disconnected.

G acts naturally on the right on \bar{M} , and hence on $L^2(\bar{M})$. This linear representation of G is analogous to the matrix representation of a finite permutation group. A finite permutation representation ρ is determined up to linear equivalence by its character χ , with $\chi(g) = \text{tr}\rho(g)$ counting the fixed points of g . The situation here should be exactly analogous, the only question being exactly how to define the character. The answer comes from the Selberg trace formula.

For now let's extend the discussion to an arbitrary unimodular Lie group G , possibly disconnected. Let $\Gamma < G$ be a discrete subgroup with compact quotient $\bar{M} = \Gamma \backslash G$. (Notice that we make no mention here of M , though in the intended application \bar{M} will arise from a homogeneous quotient $M = \Gamma \backslash G/K$.) Denote by $\text{Cl}(g, G)$ the conjugacy class of g in G , and by $Z(g, G)$ the centralizer of g in G . Introduce Haar measure ρ^g on $Z_G(g)$, normalized in a consistent (i.e., G -equivariant) way. Attribute to $\text{Cl}(\gamma, \Gamma)$ the *weight* $\rho^\gamma(Z(\gamma, \Gamma) \backslash Z(\gamma, G))$, and define the *character* $\chi_{\bar{M}}$ to be the function associating to $g \in G$ the total weight of all conjugacy classes $\text{Cl}(\gamma, \Gamma)$ for which $\text{Cl}(\gamma, G) = \text{Cl}(g, G)$. Extend the definition of $\chi_{\bar{M}}$ to $\bar{M} = \cup_j \Gamma_j \backslash G$ by linearity.

As in the finite case, the character is a *central function*, which means that $\chi_{\bar{M}}(gh) = \chi_{\bar{M}}(hg)$ for all $g, h \in G$, or what is the same, $\chi_{\bar{M}}(g)$ depends only on the conjugacy class $\text{Cl}(g, G)$. In analogy to the finite case, we can think of $\chi_{\bar{M}}(g)$ as measuring (in appropriate units) the size of the fixed point set $\{x \in \bar{M} : xg = x\}$.

Proposition 4 (Bérard). *The character $\chi_{\bar{M}}$ determines the representation $L^2(\bar{M})$ up to linear equivalence.*

Proof. Using a version of Selberg’s trace formula we can write the trace of the integral operator associated to any smooth function of compact support on G in terms of the values of the character $\chi_{\bar{M}}$. (Cf. Wallach [15, Theorem 2.1], Selberg [13, (2.10) on p. 66].) By standard representation theory, these traces determine the representation. For details, see Bérard [1]. \square

Proposition 5 (DeTurck and Gordon). *The character $\chi_{\bar{M}}$ determines the trace of any natural operator on any natural vector bundle over M .*

Proof. Selberg again. (Cf. DeTurck and Gordon [4].) \square

With this preparation, we have the following corollaries of Theorem 1.

Corollary 1 (Character is determined). *The Laplace spectrum of a hyperbolic 2-orbifold M determines the character $\chi_{\bar{M}}$.* \square

Corollary 2 (Representation-equivalence). *Laplace-isospectral hyperbolic 2-orbifolds determine equivalent representations of $\text{Isom}(H^2)$.* \square

Corollary 3 (Strong isospectrality). *If two compact hyperbolic 2-orbifolds are Laplace-isospectral then they have the same spectrum for any natural operator acting on sections of any natural bundle.* \square

10 Counterexamples

The analog of Theorem 1 fails for flat 2-orbifolds. In the connected case it does go through more or less by accident, just because there aren’t many connected flat 2-orbifolds. But there are counterexamples among disconnected flat 2-orbifolds. We described such examples briefly in [5].

Here’s our premier example, which we call *the $1/2 + 1/6 = 2/3$ example*. Let H_1 denote the standard hexagonal flat torus $\langle(1, 0), (-\frac{1}{2}, \frac{\sqrt{3}}{2})\rangle \backslash \mathbf{R}^2$. H_1 has as 2-, 3-, and 6-fold quotients a 2222 orbifold H_2 (this is a regular tetrahedron); a 333 orbifold H_3 ; and a 236 orbifold H_6 . (See Figures 7 and 8.) Spectrally,

$$H_2 + H_6 \equiv 2H_3, \tag{1}$$

meaning that these spaces have the same Laplace spectrum. (In fact, as we’ll discuss below, they are isospectral for the Laplacian on k -forms for

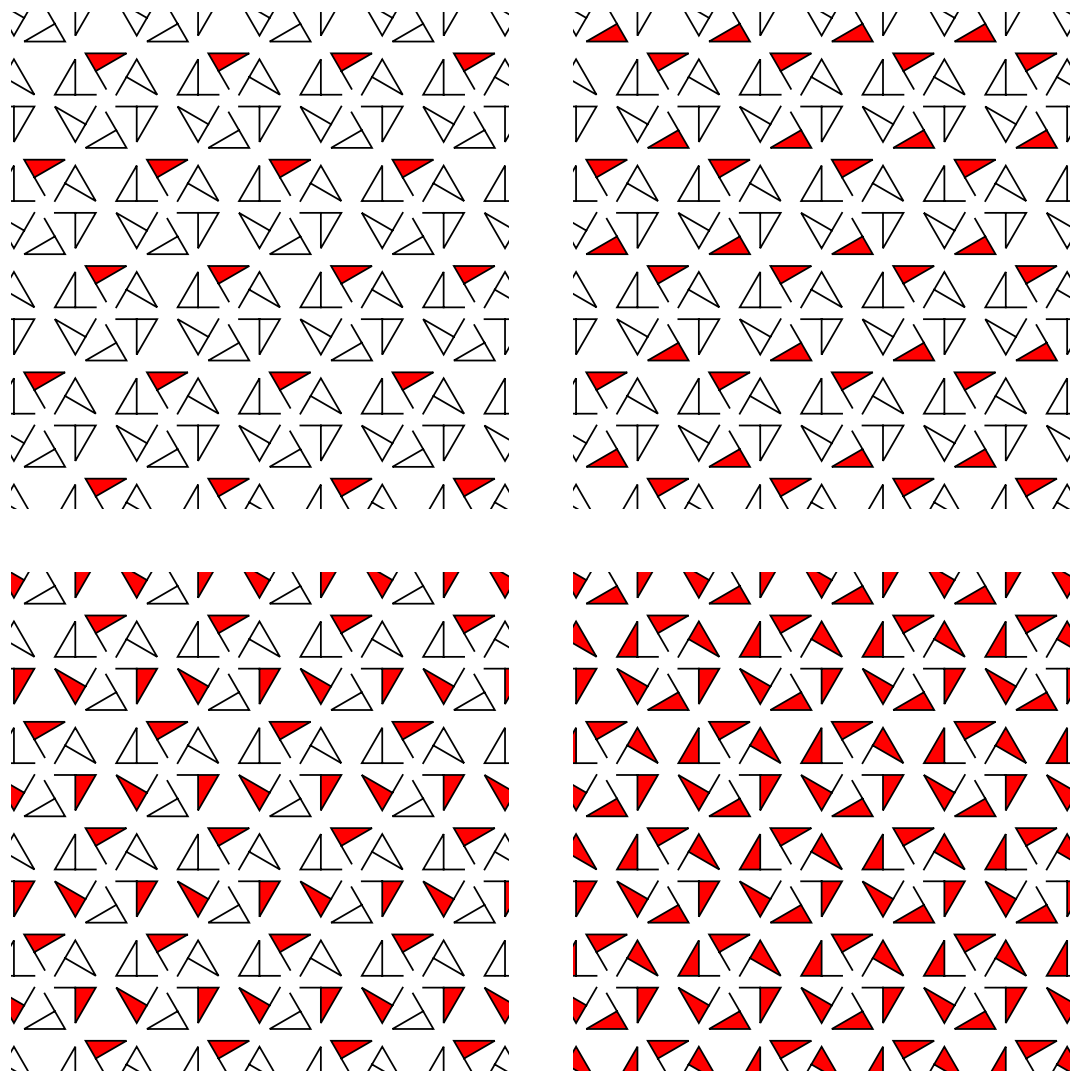


Figure 7: The universal covers of the standard hexagonal torus H_1 and its quotient orbifolds H_2 , H_3 , and H_6 .

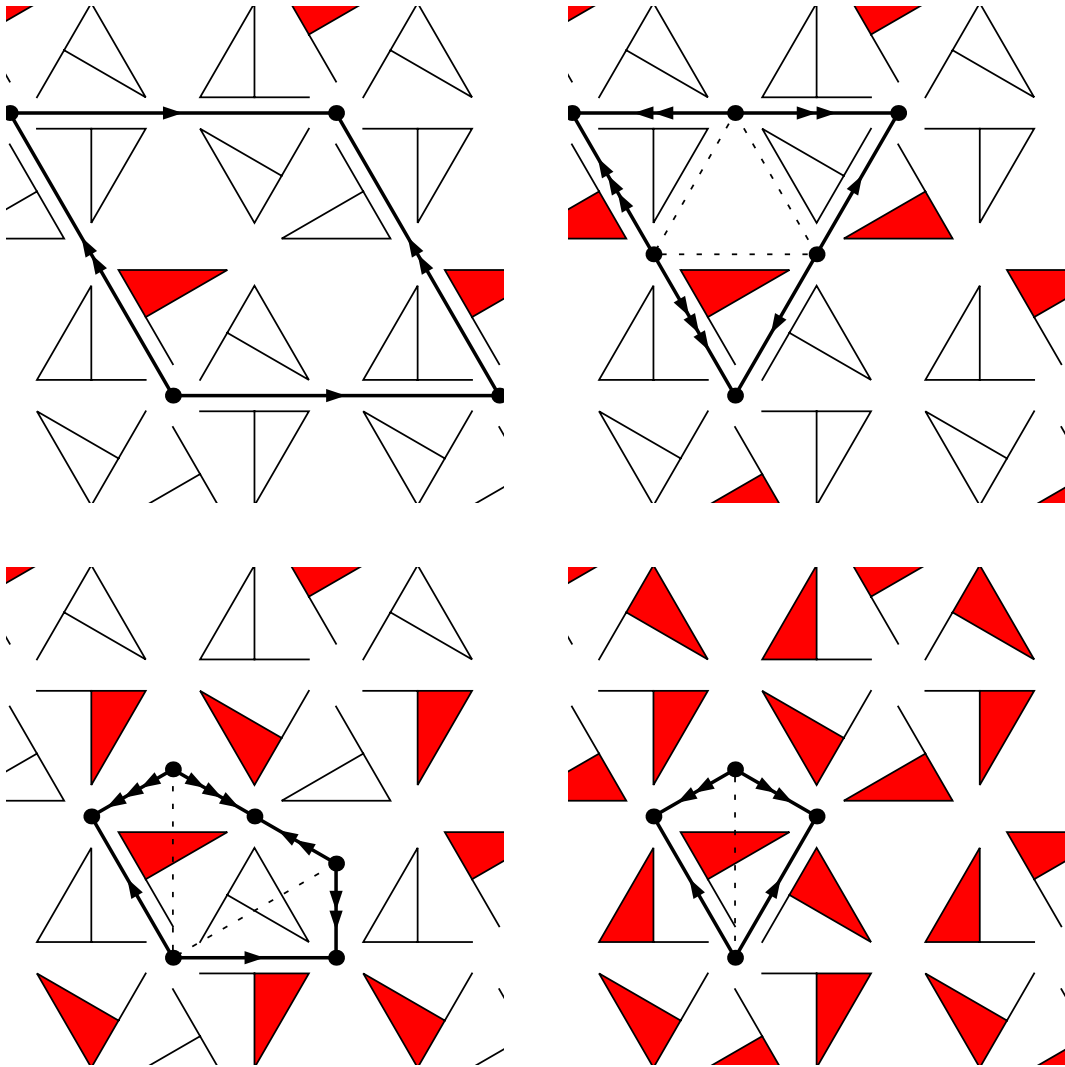


Figure 8: The orbifolds $H_1 = \circ$, $H_2 = 2222$, $H_3 = 333$, and $H_6 = 236$.

$k = 0, 1, 2$.) Of course these two spaces match as to volume ($1/2+1/6=2/3$) and number of components ($1+1=2$). But conepoints do not match. On the left we have a 2222 and a 236, so five conepoints of order 2; one of order 3; one of order 6. On the right we have two 333s, so nine conepoints of order 3.

The reason this example is possible is that in the flat case, the contributions of rotations to the counting kernel differ only by a multiplicative constant. Lumping together the contribution of all the rotations associated with a conepoint of order n , we get something proportional to $\frac{n^2-1}{n}$. (This nice simple formula was discovered by Dryden et al. [6].) For a general 2-orbifold with variable curvature, it measures the contribution of conepoints to the short-time asymptotics of the heat trace. In the flat case, the short-time asymptotics determine the entire contribution, because the contributions of all rotations are exactly proportional.

Combining contributions of all conepoints belonging to connected orbifold of various kinds, we get the following totals:

$$\begin{aligned} 2222 : & \quad 4 \cdot \frac{3}{2} = 6 \\ 333 : & \quad 3 \cdot \frac{8}{3} = 8 \\ 244 : & \quad \frac{3}{2} + 2 \cdot \frac{15}{4} = 9 \\ 236 : & \quad \frac{3}{2} + \frac{8}{3} + \frac{35}{6} = 10. \end{aligned}$$

The isospectrality $H_2+H_6 \equiv 2H_3$ arises because $6+10 = 2 \cdot 8$ makes conepoint contributions match; we've already observed that the volumes match; and geodesic contributions match because on both sides the covering manifolds are $2H_1$.

We get a second isospectrality

$$H_1 + H_3 + H_6 \equiv 3H_2$$

because $8 + 10 = 3 \cdot 6$, $1 + \frac{1}{3} + \frac{1}{6} = 3 \cdot \frac{1}{2}$, and on both sides the covering manifolds are $3H_1$.

Combining these two relations yields other Laplace-isospectral pairs, e.g.:

$$H_1 + 3H_3 \equiv 4H_2;$$

$$H_1 + 4H_6 \equiv 5H_3;$$

$$2H_1 + 3H_6 \equiv 5H_2.$$

By linearity, all these relations satisfy the condition of having equal volume, number of components, and contributions from conepoints. But look

here: We're talking, in effect, about formal combinations of H_1, H_2, H_3, H_6 , so we're in a space of dimension 4. We have three linear conditions, but to our surprise, the subspace they determine has dimension 2. Our three linear conditions are not independent. If we match volume and number of components, agreement of cone-point contributions follows for free. But why? We don't know.

A similar coincidence happens for square tori. Let T_1 denote the standard square torus $\mathbf{Z}^2 \backslash \mathbf{R}^2$. T_1 has as 2-, and 4-fold quotients a 2222 orbifold T_2 and a 244 orbifold T_4 . We're in a 3-dimensional space, so we expect to be out of luck when we impose 3-constraints, but in fact we have the relation

$$T_1 + 2T_4 \equiv 3T_2.$$

We check equality of volume $1 + \frac{2}{4} = \frac{3}{2}$ and number of components $1 + 2 = 3$, and then we find that equality of cone-point contributions follows for free: $2 \cdot 9 = 3 \cdot 6$. Again, why?

Conjecturally, up to Sunada-equivalence the relations we've given for hexagonal and square tori are all there are: See Section 12 below.

These relations apply only to the spectrum of the Laplacian on functions, not 1-forms. When we apply the Selberg formula to 1-forms, there is still interference between spectral contributions of cone-points, which allows our $1/2 + 1/6 = 2/3$ example to continue to slip through: It is isospectral for 1-forms as well as for functions. But we get additional constraints, which taken with those coming from the 0-spectrum force there to be the same number of torus components on each side, and this wipes out the other examples. The reason we have to have the same number of torus components is that this is just half the dimension of the space of 'constant' or 'harmonic' 1-forms, meaning those belonging to the 0-eigenspace of the Laplacian. And since we are expecting just one more linear constraint, this must be it. So, no additional mystery here, though when you do the computation it still seems a little surprising.

The isospectrality of the $1/2 + 1/6 = 2/3$ example does not hold for all natural operators, because the left side admits harmonic differentials that the right side does not.

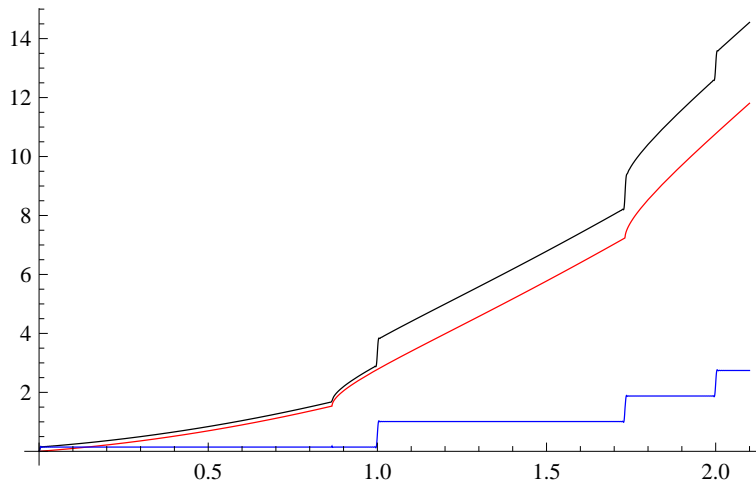


Figure 9: The counting trace for the $*333$ orbifold with side length $\frac{1}{\sqrt{3}}$, computed numerically by summing the contributions of the 11626 eigenvalues with wave number $k < 1000$. To combat the Gibbs phenomenon (also called ‘ringing’), we have used the windowing function $1 - (k/k_{\max})^2$ to reduce the contribution of the sum from larger eigenvalues. The upper line is the counting trace; the middle is the theoretical contributions from orbifold features (reflectors and boundary corners); the lower line is the difference, attributable to the identity and other translations. Observe the jump at 0; the bend at $\frac{\sqrt{3}}{2}$; the jumps at 1 and 2; the jump plus bend at $\sqrt{3}$.

11 Putting the Selberg formula to work

Here we compute the counting trace for some flat orbifolds, using the Selberg formula.

Figure 9 shows a plot of the counting trace of a $*333$ orbifold, computed approximately from the Laplace spectrum. We can think of $*333$ as an equilateral triangle with Neumann boundary conditions. We have chosen the side length to be $\frac{1}{\sqrt{3}}$, so that the covering torus is a standard hexagonal torus with shortest geodesics of length 1. The shortest geodesic in the quotient $*333$ is the 3-bounce geodesic in the middle, which has length $\frac{\sqrt{3}}{2}$. Next shortest are the torus geodesics of length 1. Then at length $\sqrt{3}$ we get the second power of the middle geodesic, which is orientation preserving and hence a torus geodesic, plus geodesics parallel to the boundary, which count as both orientation-preserving and orientation-reversing.

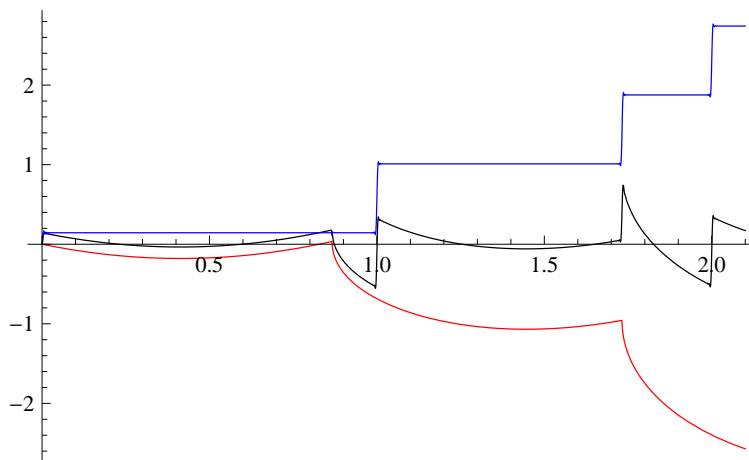


Figure 10: The counting trace of an equilateral triangle with side length $\frac{1}{\sqrt{3}}$, with Dirichlet boundary conditions.

Figure 10 shows another plot of the counting kernel as reconstructed from the Laplace spectrum. This time the space is an equilateral triangle with Dirichlet boundary conditions. Such a space is a generalized orbifold, whose functions change sign under some deck transformation (in this case, just those which reverse orientation). Kelvin in effect worked in such a space when computing the field of a point charge near an infinite conducting planar boundary. The counting kernel counts images with sign ± 1 . Note that we see the same jumps and bends as in the Neumann case above, only now the bends are downward rather than upward.

Now let's try computing the counting trace of a nonorbifold triangle, using the same formula as for orbifolds. This can be justified by defining the counting kernel to be the Green's function for a variant of the wave equation that we may call the *counting wave equation*. Figure 12 shows Neumann and Dirichlet counting trace plots for an equilateral triangle with angles $\frac{\pi}{5}, \frac{\pi}{5}, \frac{3\pi}{5}$ (side lengths $1, 1, \phi$). Because we are using fewer eigenvalues than in the graphs above, the bends and jumps are less distinct here. It would be great to have more eigenvalues, but these are surprisingly hard to come by! The 611 Neumann eigenvalues and 591 Dirichlet eigenvalues used here were kindly supplied by Alex Barnett.

In a non-orbifold triangle we expect bends in the counting trace graphs corresponding to orbits that are diffracted at the non-orbifold vertices. For

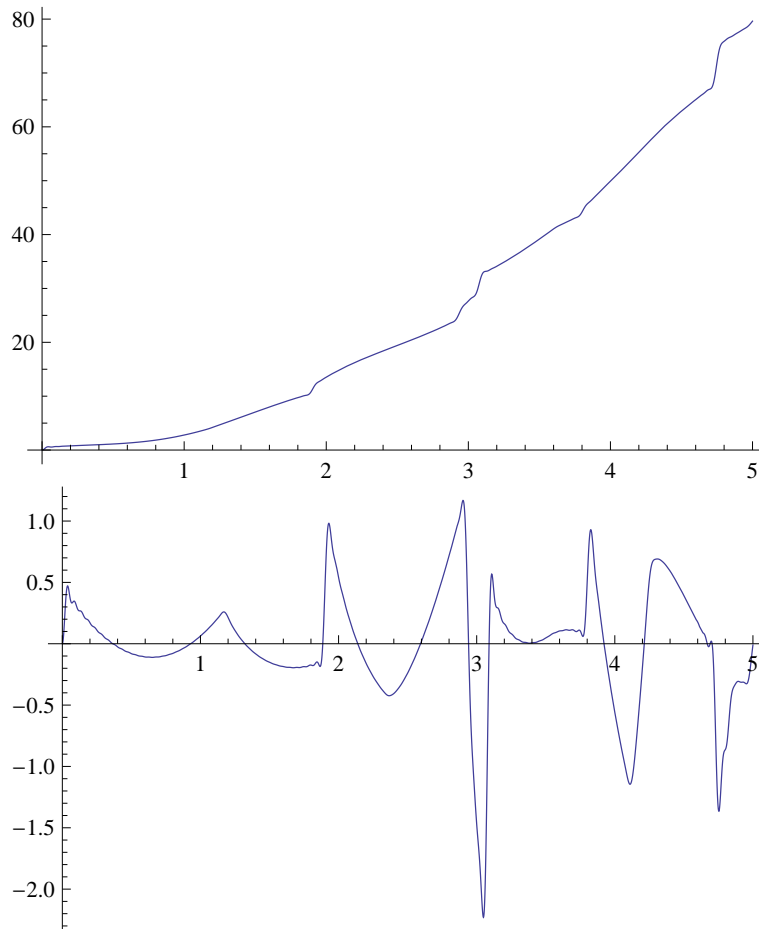


Figure 11: The Neumann and Dirichlet counting traces for a triangle with angles $\frac{\pi}{5}, \frac{\pi}{5}, \frac{3\pi}{5}$ and sides $1, 1, \phi$. 611 Neumann and 591 Dirichlet eigenvalues courtesy of Alex Barnett.

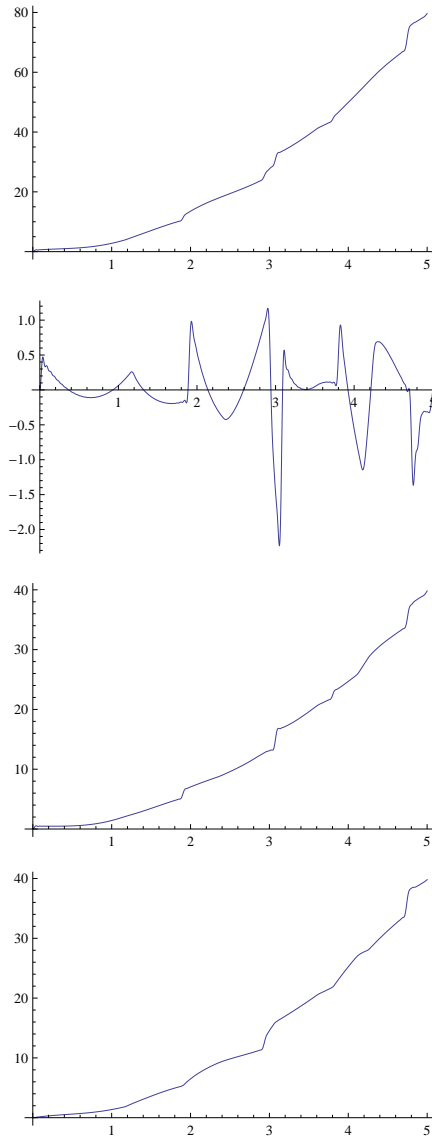


Figure 12: The Neumann and Dirichlet counting traces from Figure 11, together with their average and half their difference.

example, here we see a bend at length $2 \sin \frac{\pi}{5}$, corresponding to the orbit that goes back and forth between the $\frac{3\pi}{5}$ vertex and the midpoint of the opposite edge. (This is most visible in the Dirichlet graph, but it is present in the Neumann graph as well.) You might enjoy identifying the closed orbits that are the source of the other bends and jumps that are visible in these graphs.

Note. Three of the four graphs in Figure 12 appear to be increasing, just as they would be in the case of an orbifold. We don't know if these curves really are monotonic, and if so, whether this illustrates a general phenomenon. To investigate this, we will want to know how a counting wavefront diffracts when it encounters a non-orbifold vertex. We could try some numerical experiments, if we had eigenfunctions to go along with our list of eigenvalues. Alternatively, we could try using the analog for counting waves of Sommerfeld's explicit formula for the Green's function of the classical wave equation in a wedge.

12 Conjectures

As we observed in section 10, we conjecture, or at least hypothesize, that the only spectral relations between flat orbifolds beyond those coming from Sunada's method are those relations we have found for hexagonal and square tori; of course these come in all sizes. Now, at this point, Peter doesn't remember checking orbifolds with reflectors, though he can't imagine why he wouldn't have. But, the hard thing here is not going to be dealing with relations between orbifolds. There are two real issues. The first is to see that any isospectrality breaks apart into commensurable pieces. The second is going to be dealing with the case of tori. Specifically, it seems like for tori, the only relations should be those implicit in the theory of Hecke operators. The simplest example of a Hecke relation is the isospectrality between 'two 1-by-1s and a 2-by-2; two 2-by-1s and a roo-by-roo'. Here 'roo' is my (Peter's) proposed abbreviation for 'the square root of two'.

Moving now to the hyperbolic case, Theorem 1 implies that all hyperbolic triangular orbifolds $*abc$ (e.g. $*237$) are determined by their Laplace spectrum. It seems likely that all hyperbolic quadrilateral and pentagonal orbifolds are also determined. Note that in light of Theorem 1, we can treat this as a purely geometrical question. This question could most likely be settled by a computer-aided investigation, along the lines of the computer-aided proof that flat 3-tori are determined by their Laplace spectrum. We can ex-

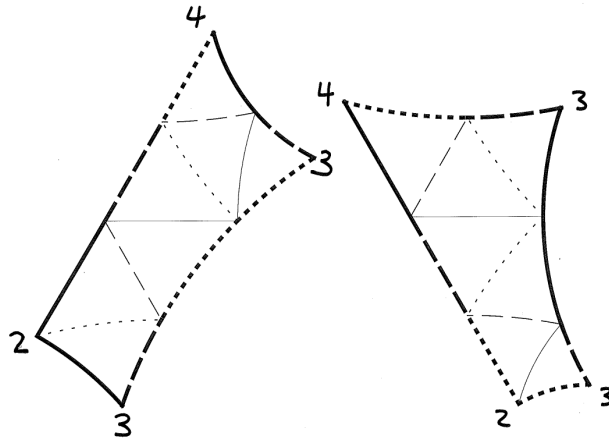


Figure 13: An isometric pair of type $*2334$, from glueing pattern 7(3).

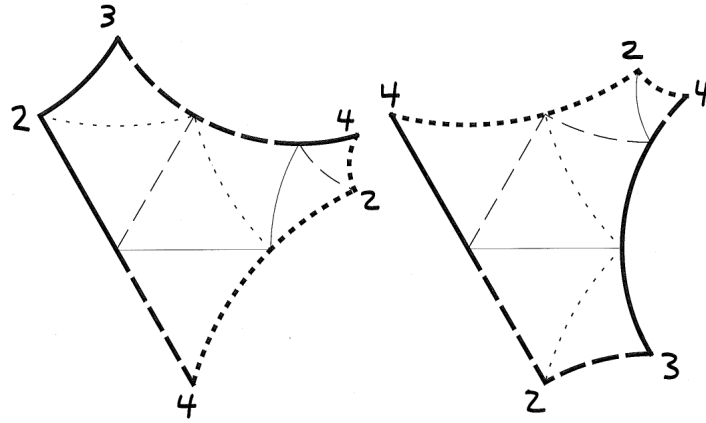


Figure 14: An isometric pair of type $*23424$, from glueing pattern 7(2).

pect complications in the neighborhood of the isometric pairs of quadrilateral and pentagonal orbifolds to which the seven-triangle pairs 7(3) and 7(2) of Appendix A degenerate when the triangles are made too symmetrical. (See Figures 13 and 14.)

This is exactly the kind of issue Rich Schwartz and Pat Hooper faced down in the proof of the ‘100 degree theorem’ [11] [12], which states that any flat triangle with no angle larger than 100 degrees has a closed billiard trajectory. So maybe that investigation would be a better guide here than

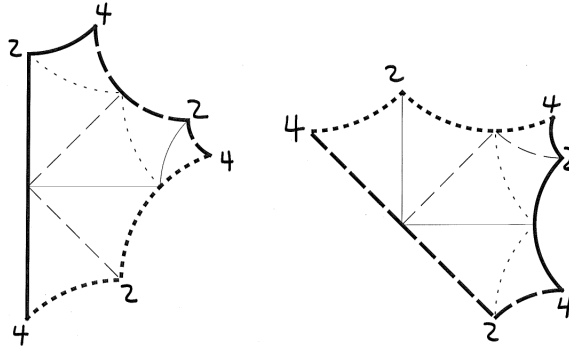


Figure 15: An isometric pair of type $*242424$, from glueing pattern 7(1). Note that this orbifold has 3-fold symmetry, as its Conway symbol suggests (but does not imply).

the business about 3-tori. We hope that this problem will turn out to be much easier than the billiard problem.

It seems likely that the hexagons of Figure 1 constitute the simplest isospectral pair of hyperbolic hexagonal orbifolds, and possible that all such pairs arise from the glueing diagram 7(1). In trying to prove this we can expect problems in the neighborhood of the isometric pair we get from glueing pattern 7(1). (See Figure 15.) Another problematic pair arises from pattern 13a(5).

A similar computer-assisted approach might show that hyperbolic surfaces of genus 2 and 3 are determined by their Laplace spectra, as suggested by Bob Brooks. Here again there is an obvious to expect difficulties, where a degenerate Sunada pair yields isometric surfaces.

One more thing: It seems likely that in any dimension, if two hyperbolic (or spherical) orbifolds are isospectral on k -forms for all k , then they are representation-equivalent. Pesce [10] showed that that representation-equivalence follows from isospectrality for all natural self-adjoint elliptic differential operators on natural bundles. In formulating his result, Pesce simply says that representation equivalence follow from isospectrality of all natural operators; if you allow non-self-adjoint operators, the problem becomes much easier, because representation-equivalence just amounts to isospectrality for

the regular action of G on functions on G , and a function on G is a section of a natural bundle over $\Gamma \backslash G$. Here we are hoping to make do with only the Laplacian on forms. What made Peter think this would be doable is that fact that for 2-orbifolds, if you know the spectrum on functions and 1-forms, you can simply read off the character χ , using an extension of the ‘hard side’ of Selberg’s formula to sections of bundles that are not flat. This works in the 2-dimensional case, where it turns out that if you know the spectrum of the Laplacian on functions and on 1-forms, you can just ‘read off’ the character without all the difficulty you face when you try to use functions alone. (This is the difficulty that never really arose in this paper, since we outsourced the crux of the argument to our earlier paper on nonorientable hyperbolic 2-manifolds.) The issue comes down to this: Is an eigenfunction of the Laplacian on a k form automatically an eigenfunction for the averaging operator where you restrict the form to a ball in the universal cover H^n and translate the values back to the center of the ball using the exponential map? If this is false, as it may well be when $n > 2$, then the problem could be harder than Peter had imagined.

Appendix: Conway’s quilts

In this section we reproduce John Conway’s catalog of transplantable pairs coming from small projective groups. Conway generated these pairs using his theory of quilts, while Peter watched admiringly.

The 16 pairs of sizes 7, 13, and 15, which are treelike and thus give planar isospectral domains, were reported in Buser et al. [2]. In [2] we also presented the first of the size 21 pairs, which yields planar isospectral domains for certain triangle shapes. (The second of these size 21 pairs can also yield planar domains, so despite what some authors have mistakenly concluded, is no special role for the number 17 here.) The rest of these examples have been languishing on my webpage.

There is much to be said about these examples and where they come from, but as our purpose here is mainly to bring them to light, we make just a few remarks.

A transplantable pair can be thought of as arising from a pair of finite permutation actions of the free group on generators a, b, c . These actions are equivalent as linear representations but (if the pair is to be of any use) not as permutation representations. In the examples at hand, each representing

permutation is an involution, so these representations factor through the quotient $F = \langle a, b, c : a^2 = b^2 = c^2 = 1 \rangle$, the free product of three copies of the group of order 2.

From any transplantable pair we can get other pairs through the process of braiding, which amounts to precomposing the permutation representations with automorphisms of F , called L and R :

$$L : (a, b, c) \mapsto (aba^{-1}, a, c);$$

$$R : (a, b, c) \mapsto (a, c, cbc^{-1}).$$

Left-braiding a permutation representation ρ can be viewed as first conjugating $\rho(b)$ by $\rho(a)$, i.e. applying the permutation $\rho(a)$ to each index in the cycle representation of $\rho(b)$, and then switching $\rho(a)$ with the new $\rho(b)$. Right-braiding is the same, only with c taking over the role of a .

Pairs of permutations that are equivalent in this way belong to the same *quilt*. We identify pairs that differ only by permuting a, b, c , or by reversing the pair. A quilt has extra structure which we are ignoring here: See Conway and Hsu [3]. This structure makes it easier to understand and enumerate the pairs. But the computer has no trouble churning out pairs belonging to the same quilt.

In the diagrams to follow, the permutations corresponding to a, b, c are represented by dotted, dashed, and solid lines. Thin lines connect elements that are interchanged, while thick lines delimit fixed points. Thick lines in the interior of the diagram separate points that are each fixed, rather than interchanged. Sometimes thin lines occur on the boundary of the diagram, which means that the boundary must be glued up. We have taken care to lay out the diagrams so that there is at most one pair of thin boundary lines of each type (dotted, dashed, or solid), so that even without the usual glueing arrows there is no ambiguity of how the boundary is to be glued up.

The label below a pair tells the sequence of braiding operations that gets you this pair from the first pair of the quilt. The labels read left-to-right, so that $\{L, L, R, L\}$ means two lefts, a right, then another left. In most but not all cases, the quilt has been explored in ‘left-first search’ order.

To refer to these pairs, we will write 7(1) for the first pair of quilt 7, 13a(5) for the fifth pair of quilt 13a, etc. As this is not very canonical, we reserve the right to replace the parenthesized number by a list (possibly empty) of L s and R s, so that for example 13a(5) would become 13aLLRL, and 7(1) would become simply 7.

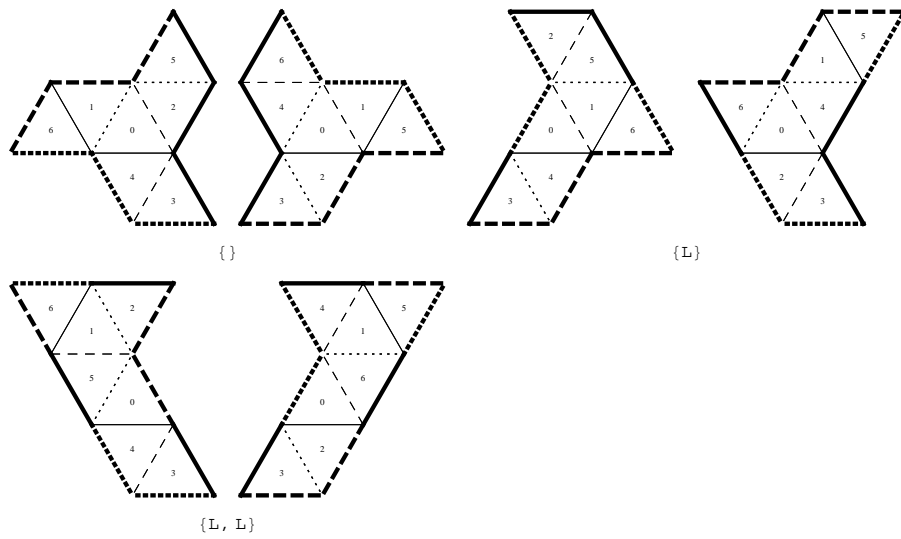


Figure 16: Quilt 7

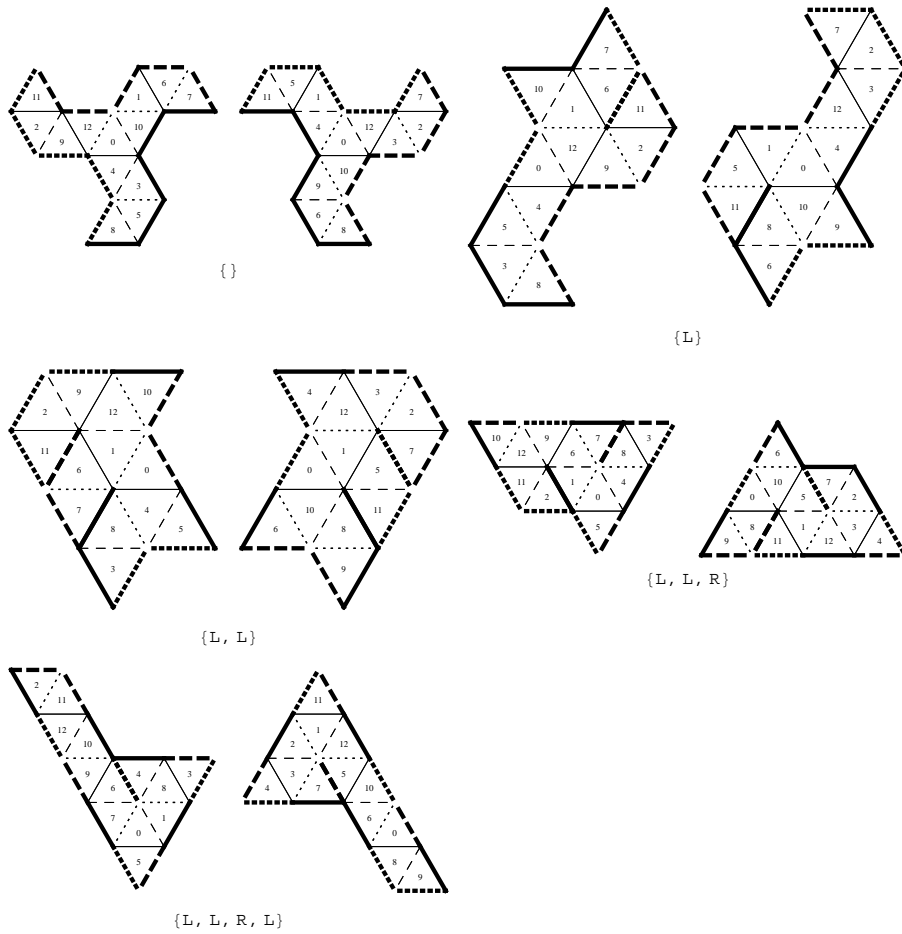


Figure 17: Quilt 13a

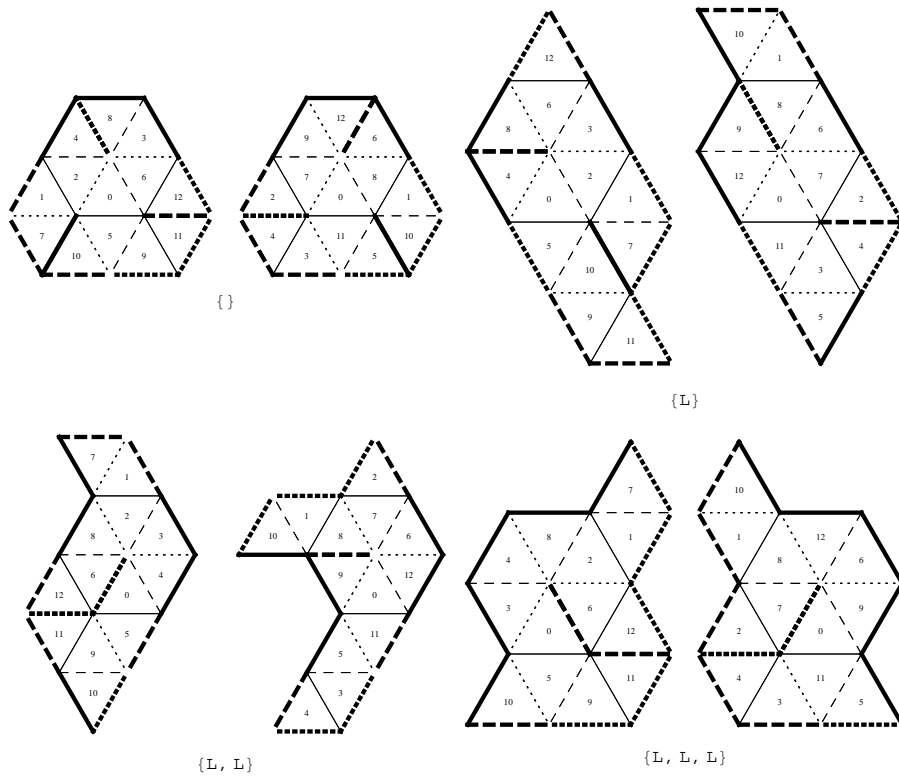


Figure 18: Quilt 13b

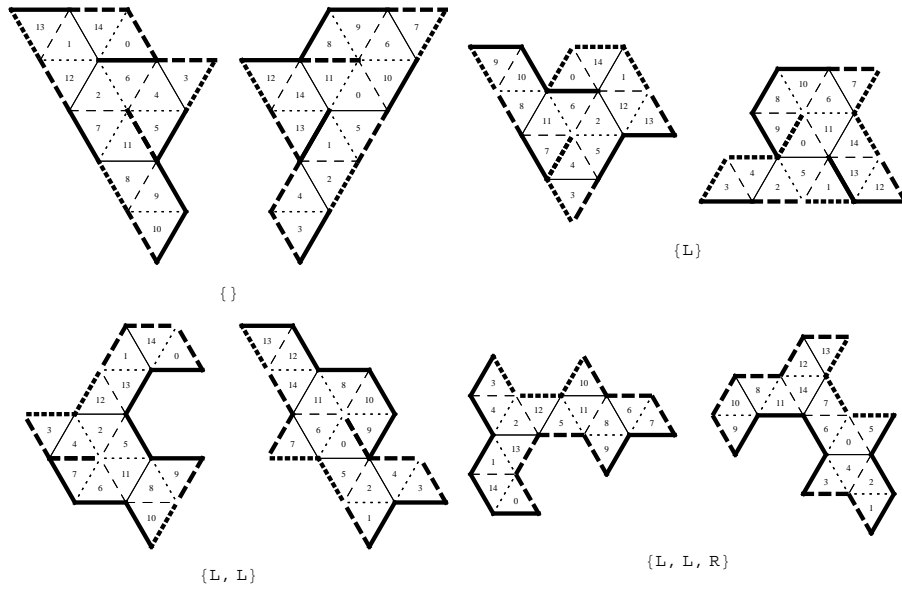


Figure 19: Quilt 15

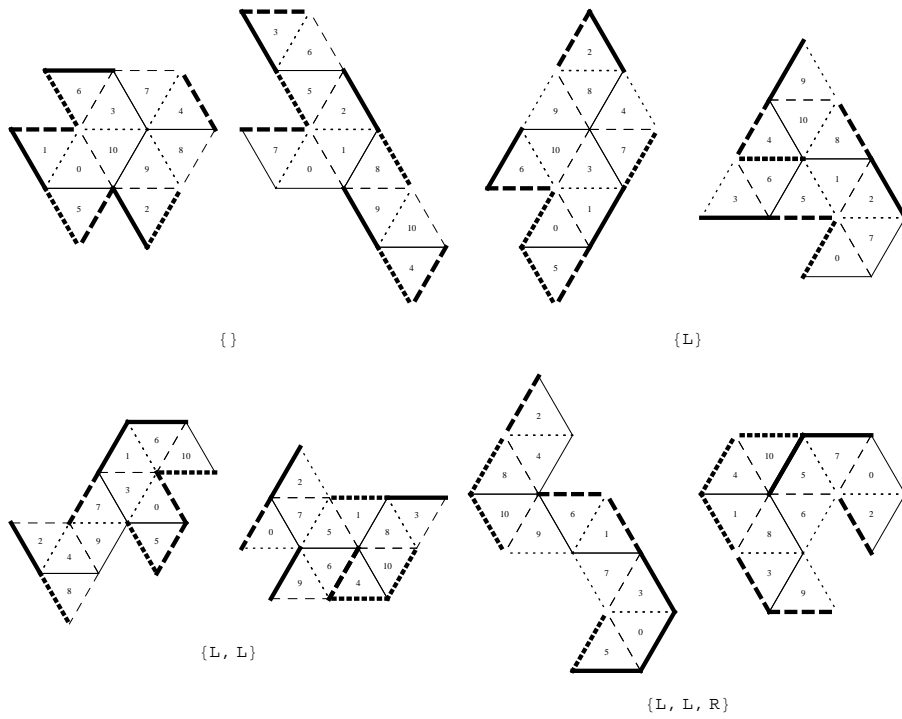


Figure 20: Quilt 11f

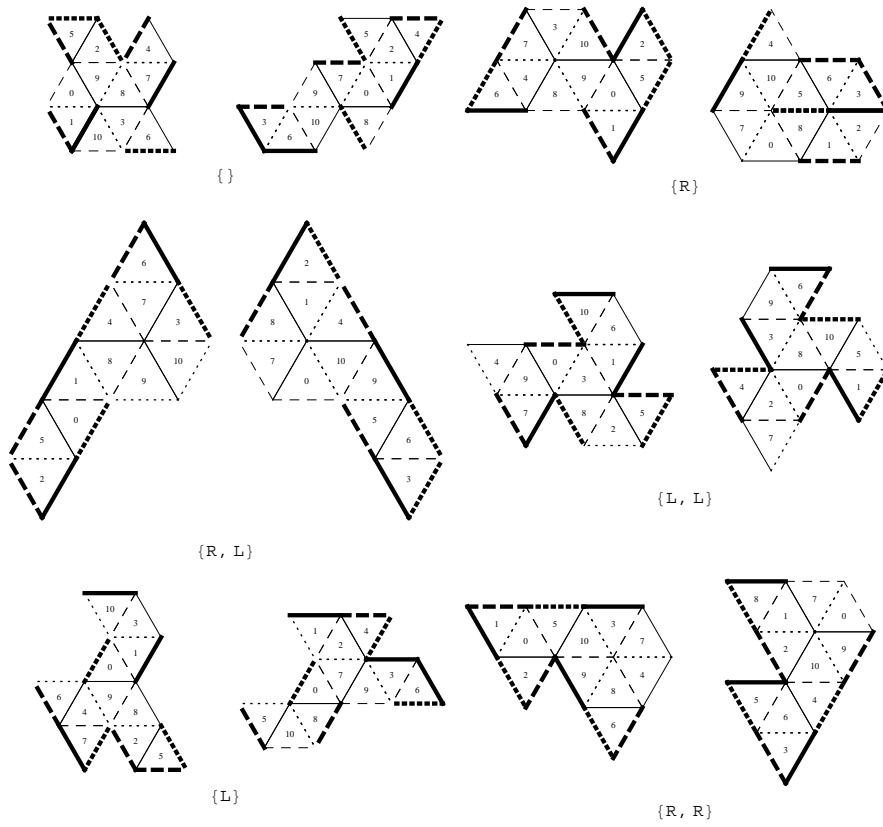


Figure 21: Quilt 11g

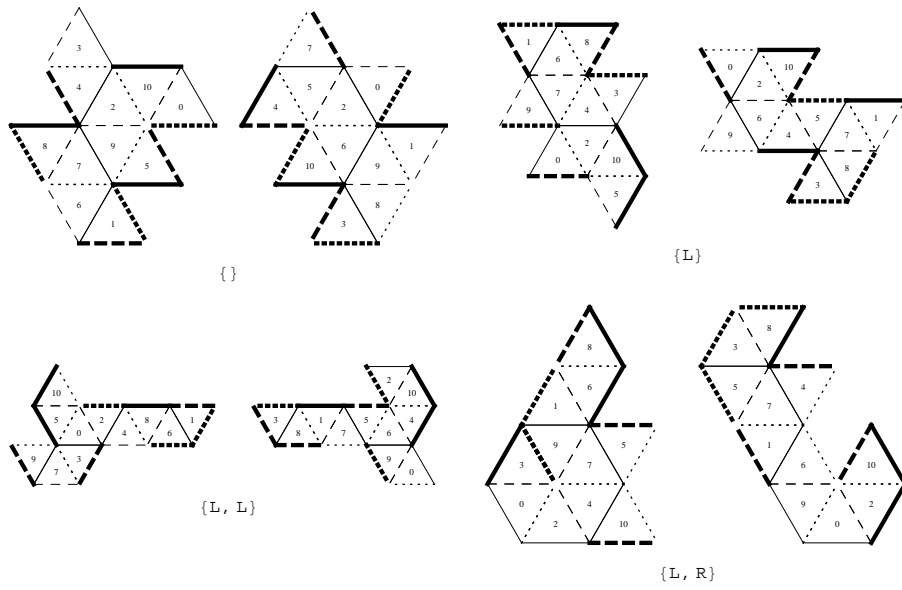


Figure 22: Quilt 11h

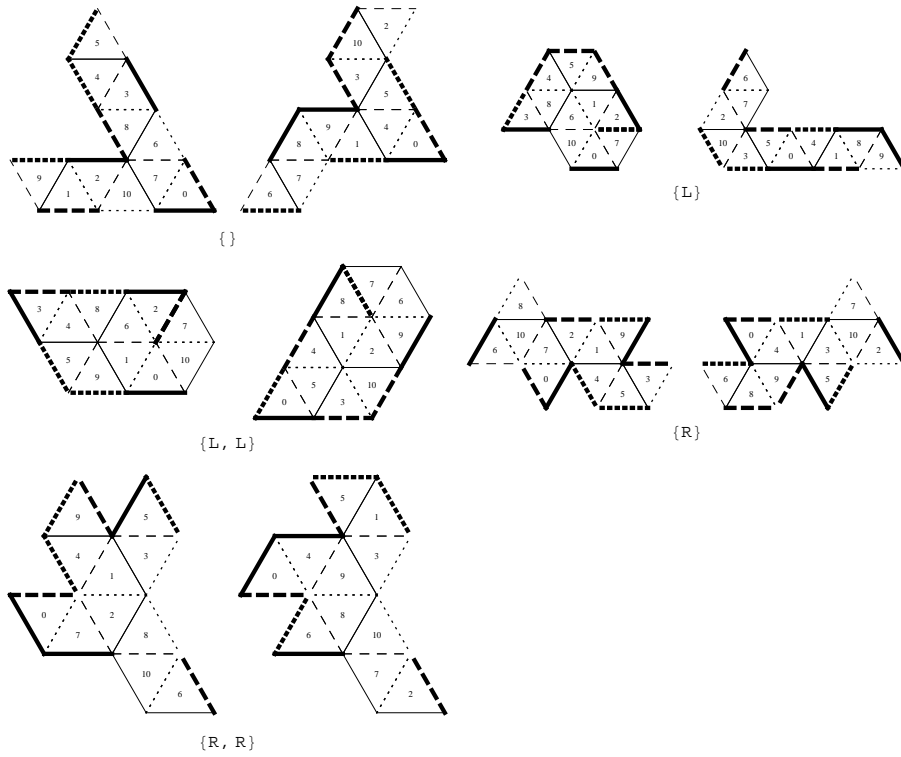


Figure 23: Quilt 11i

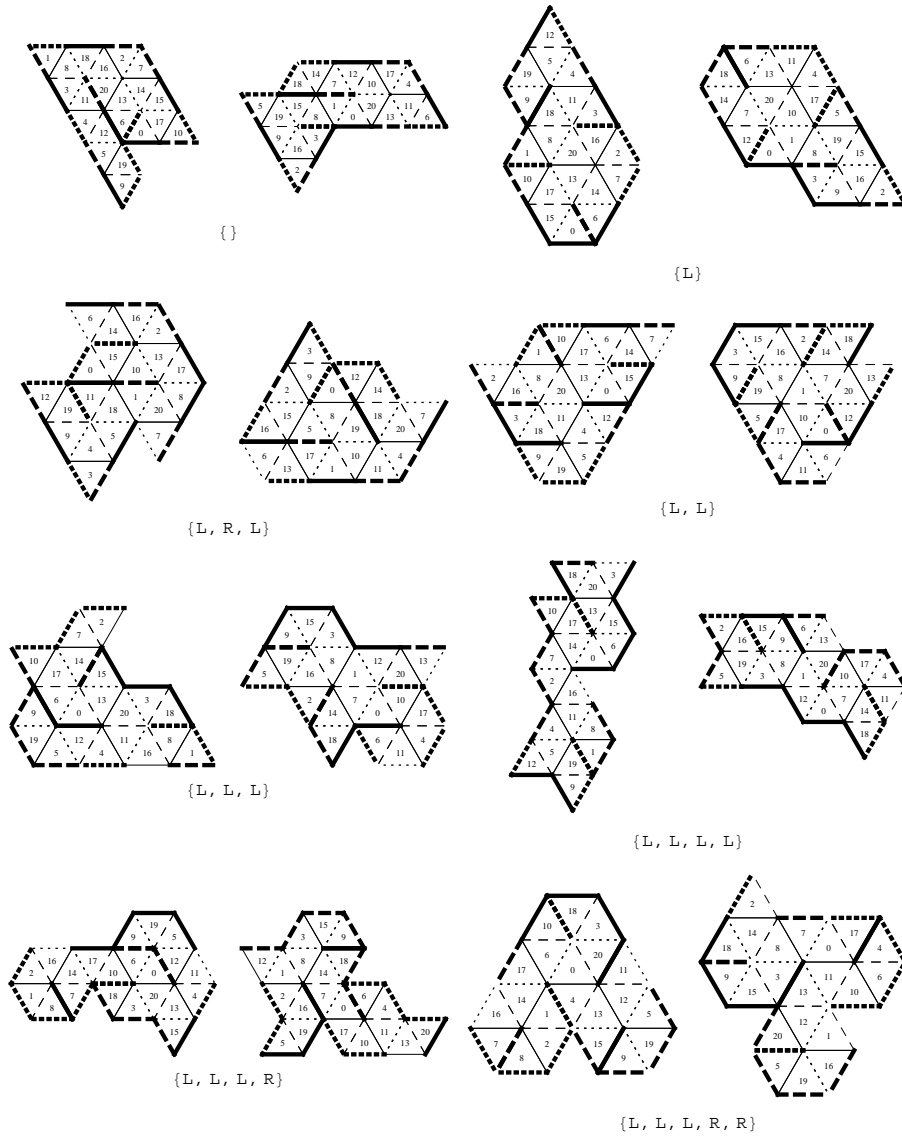


Figure 24: Quilt 21

For historical reasons, the four quilts of size 11 are called $11f$, $11g$, $11h$, $11i$.

Acknowledgements

We are grateful to Alex Barnett for supplying the spectral data for non-orbifold triangles that we used in section 11, and for much helpful advice about waves and the like.

References

- [1] Pierre Bérard. Transplantation et isospectralité. II. *J. London Math. Soc. (2)*, 48(3):565–576, 1993.
- [2] Peter Buser, John Conway, Peter Doyle, and Klaus-Dieter Semmler. Some planar isospectral domains. *Internat. Math. Res. Notices*, 9:391ff., approx. 9 pp. (electronic), 1994.
- [3] John H. Conway and Tim Hsu. Quilts and T -systems. *J. Algebra*, 174(3):856–908, 1995.
- [4] Dennis M. DeTurck and Carolyn S. Gordon. Isospectral deformations. II. Trace formulas, metrics, and potentials. *Comm. Pure Appl. Math.*, 42(8):1067–1095, 1989. With an appendix by Kyung Bai Lee.
- [5] Peter G. Doyle and Juan Pablo Rossetti. Isospectral hyperbolic surfaces have matching geodesics, 2008, arXiv:math/0605765v2 [math.DG].
- [6] Emily B. Dryden, Carolyn S. Gordon, and Sarah J. Greenwald. Asymptotic expansion of the heat kernel for orbifolds, 2008.
- [7] Emily B. Dryden and Alexander Strohmaier. Huber’s theorem for hyperbolic orbisurfaces, 2005, arXiv:math.SP/0504571.
- [8] C. Gordon, D. Webb, and S. Wolpert. One cannot hear the shape of a drum. *Bull. Amer. Math. Soc.*, 27:134–138, 1992.
- [9] Heinz Huber. Zur analytischen Theorie hyperbolischen Raumformen und Bewegungsgruppen. *Math. Ann.*, 138:1–26, 1959.
- [10] Hubert Pesce. Variétés hyperboliques et elliptiques fortement isospectrales. *J. Funct. Anal.*, 134(2):363–391, 1995.

- [11] Richard Evan Schwartz. Obtuse triangular billiards. I. Near the $(2, 3, 6)$ triangle. *Experiment. Math.*, 15(2):161–182, 2006.
- [12] Richard Evan Schwartz. Obtuse triangular billiards. II. One hundred degrees worth of periodic trajectories. *Experiment. Math.*, 18(2):137–171, 2009.
- [13] Atle Selberg. Harmonic analysis and discontinuous groups in weakly symmetric Riemannian spaces with applications to Dirichlet series. *J. Indian Math. Soc. B*, 20:47–87, 1956. Reprinted in [14].
- [14] Atle Selberg. Harmonic analysis and discontinuous groups in weakly symmetric Riemannian spaces with applications to Dirichlet series. In *Collected Papers, vol. 1*, pages 423–463. Springer, 1989.
- [15] Nolan R. Wallach. On the Selberg trace formula in the case of compact quotient. *Bull. Amer. Math. Soc.*, 82(2):171–195, 1976.